# Measurement of the CP Asymmetry of $D^0 \rightarrow K_s K_s$ decay (Belle + Belle II)

Kavita Lalwani[1], Sanjeeda Bharati Das[1], Angelo Di Canto[2]
[1]MNIT Jaipur, India, [2]BNL, USA

17th International Conference on Interconncetions between Partcile Physics and Cosmology
14 – 18 October 2024

# Physics Motivation

- $D^0 \rightarrow K_s K_s$ is a Singly Cabibbo Suppressed (SCS) decay, which involves the interference of $c\bar{u} \rightarrow s\bar{s}$ and $c\bar{u} \rightarrow d\bar{d}$ transitions.

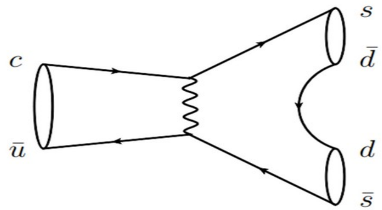


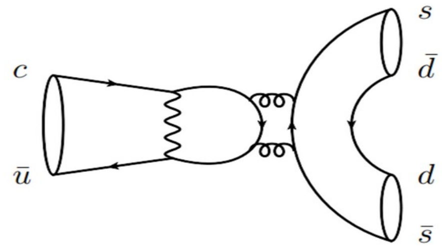


- Due to this interference, the CP Asymmetry ($A_{CP}$) may be enhanced to an observable level within the Standard Model.

- The world-average determination of $A_{CP}(D^0 \rightarrow K_s K_s)$: $(-1.9 \pm 1.0)\%$, is limited by the statistical precision.

- The world average is dominated by measurements from **Belle** and **LHCb**:
  - Using 921fb$^{-1}$ and $D^0 \rightarrow K_s\pi^0$ as the control mode, Belle measured
    $A_{CP}(D^0 \rightarrow K_s K_s) = (-0.02 \pm 1.53\ (\text{stat.}) \pm 0.02(\text{syst.}) \pm 0.17\ (\text{control mode}))\ \%$ **[Phys. Rev. Lett. 119 171801]**
  - A more precise result of $A_{CP}$ is obtained by LHCb with $D^0 \rightarrow K^+K^-$ as the control mode :
    $A_{CP}(D^0 \rightarrow K_s K_s) = (-3.1 \pm 1.2\ (\text{stat.}) \pm 0.4\ (\text{syst.}) \pm 0.2\ (\text{control mode}))\%$ **[Phys. Rev. D 104, L031102]**

- The measurement of $A_{CP}(D^0 \rightarrow K^+K^-)$ has been recently improved by LHCb bringing the corresponding uncertainty below the 0.1% level **[Phys. Rev. Lett. 131, 091802]**

➡**Goal of this analysis is to measure the time integrated Asymmetry ($A_{CP}$) in $D^0 \rightarrow K_s K_s$ Decays using $D^0 \rightarrow K^+K^-$ as the control mode, with Belle and Belle II data.**

# Time Integrated CP Asymmetry ($A_{cp}$)

- Time integrated $A_{CP}$ is defined as: $A_{CP} \equiv \frac{\Gamma(D^0 \to K_S^0 K_S^0) - \Gamma(\bar{D}^0 \to K_S^0 K_S^0)}{\Gamma(D^0 \to K_S^0 K_S^0) + \Gamma(\bar{D}^0 \to K_S^0 K_S^0)}$ *$\Gamma$ = partial decay width*

- Experimentally we measure the quantity of raw asymmetry ($A_{raw}$), defined as:

$$A_{raw} \equiv \frac{N(D^0) - N(\bar{D}^0)}{N(D^0) + N(\bar{D}^0)}$$

*$N(D^0)$ = measured yield of $D^{*+} \to D^0\pi^+$, $D^0 \to K_S K_S$ decays*
*$N(\bar{D}^0)$ = measured yield of $D^{*-} \to \bar{D}^0\pi^-$, $\bar{D}^0 \to K_S K_S$ decays*

$$A_{raw} \approx A_{FB}^{D^{*+}} + A_{CP} + A_\varepsilon^{\pi_s}$$

$A_\varepsilon^{\pi_s}$ = *asymmetry of the detection efficiency of the slow pion*

$A_{FB}$ = *forward backward asymmetry*

$$\boxed{A_{CP}^{K_s K_s} = (A_{raw}^{K_s K_s} - A_{raw}^{KK}) + A_{CP}^{KK}}$$

*Assuming that the distributions of cosθ and momenta for $D^{*+}$ and $\pi_s$ are in agreement, due to which, corresponding $A_{FB}$ and $A_\varepsilon$ cancel.*

$$A_{CP}(D^0 \to K^+K^-) = \underbrace{A_{CP}^{dir}(D^0 \to K^+K^-)}_{\text{direct CP Asymmetry}} + \underbrace{\Delta Y}_{\text{asymmetry from CP violation in mixing and in the interference between mixing and decay}} = (6.7 \pm 5.4) \times 10^{-4}$$

*direct CP Asymmetry*
***Phys. Rev. Lett. 131 (2023) 091802***

*asymmetry from CP violation in mixing and in the interference between mixing and decay*
***Phys. Rev. D104 (2021) 072010***

# Experimental facility Belle and Belle II @ KEK, Japan

Instantaneous luminosity: 2.11 x $10^{34}$ $cm^{-2}s^{-1}$ (June 2009, world record)

Dataset: 1$ab^{-1}$

Nucl. Instrum. Methods Phys. Res, Sect. A 479, 117 (2002)

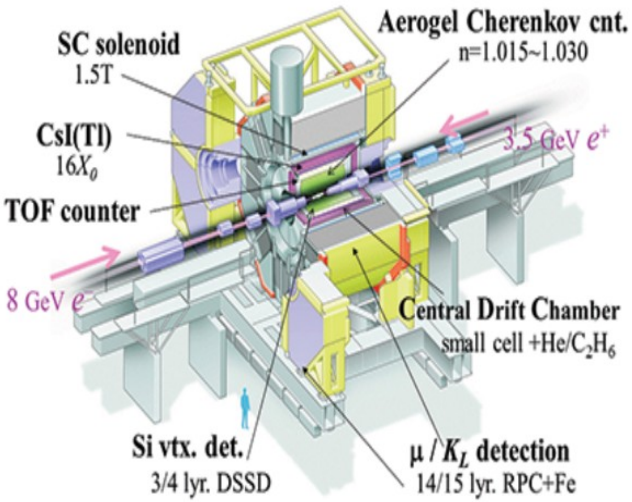


Prog. Theor. Exp. Phys. 2019, 123C01

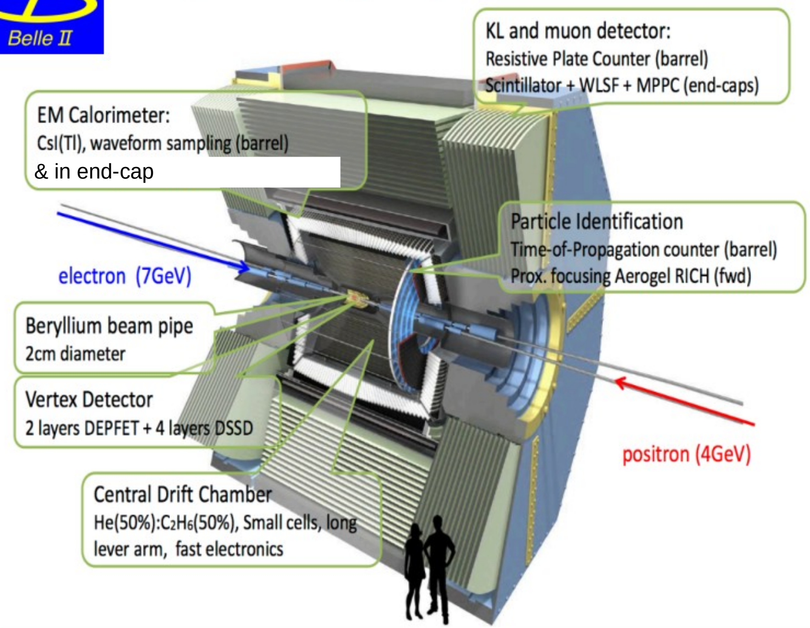


Target dataset: 50 $ab^{-1}$

Collected till date: 428 $fb^{-1}$

Instantaneous luminosity: 4.7 x $10^{34}$ $cm^{-2}s^{-1}$ (June 2022, current world record)

Used data sample collected at 427 $fb^{-1}$ by Belle II (before LS1)

**Measurement of the integrated luminosity of data samples collected during 2019-2022 by Belle II experiment arXiv:2407.00965(hep-ex)**

# $D^0 \to K_s K_s$

## Selection Criteria

| Variable | Criteria |
|---|---|
| $\lvert d_r(\pi_s)\rvert$ | $< 0.5$ cm |
| $\lvert d_z(\pi_s)\rvert$ | $< 2$ cm |
| $\theta(\pi_s)$ | $[17, 150]^\circ$ |
| $m(\pi^+\pi^-)$ | $[0.45, 0.55]$ GeV/$c^2$ |
| $m(K_S^0 K_S^0)$ | $[1.85, 1.89]$ GeV/$c^2$ (Belle) or $[1.85, 1.88]$ GeV/$c^2$ (Belle II) |
| $\Delta m$ = (m(D*+) - m(D0)) | $< 0.16$ GeV/$c^2$ |
| $p_{\mathrm{cms}}(D^{*+})$ | $> 2.5$ GeV/$c$ |
| `TreeFitter` probability | $> 0.001$ |
| Best-candidate selection | $D^{*+}$ candidate with largest `TreeFitter` probability |

(Selection criteria on Impact parameters)

(To reduce the events where $D^{*+}$ coming from B meson)

Treefitter is used with $K_s$ mass constraint and IP constraint

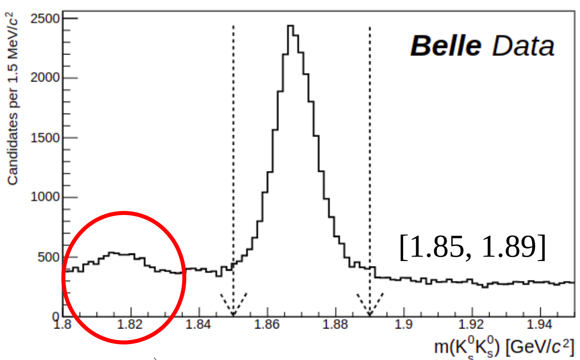


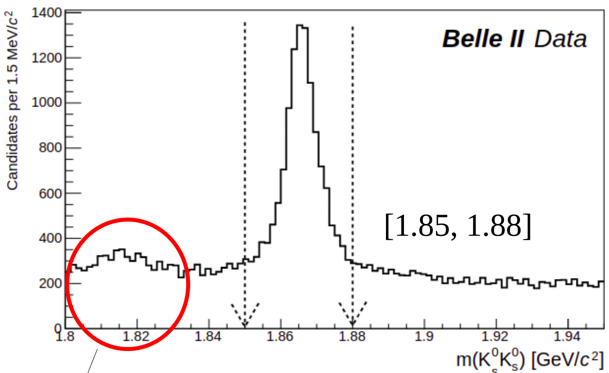


$D_s \to K_s K_s \pi^+$ ($\mathcal{B} = 7.7\times10^{-3}$), in which the charged pion acts as soft pion candidate.

$D^0 \to 2\pi^+ 2\pi^-$ is negligible and the only remaining physics background is $D^0 \to K_S \pi^+\pi^-$

# The background rejection variable $S_{min}$

$D^0 \rightarrow K_s K_s$

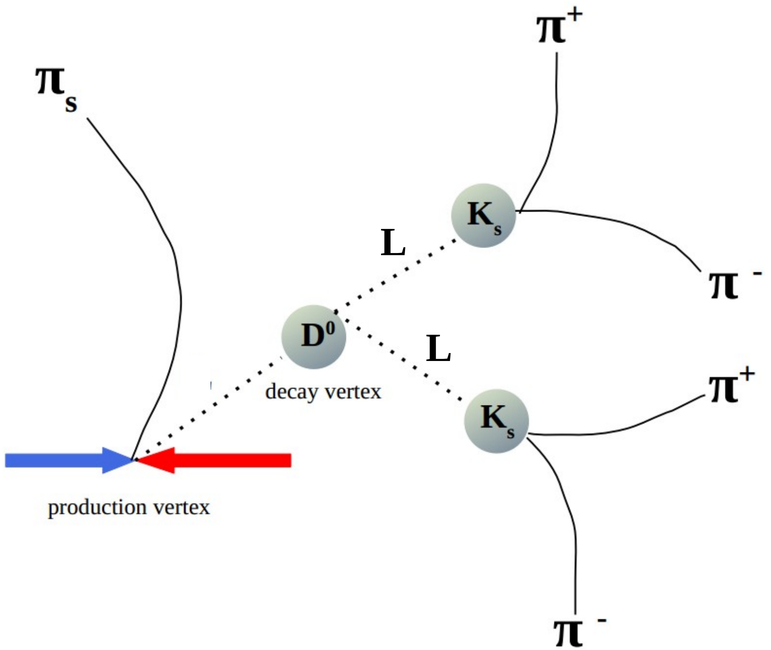


$D^0 \rightarrow K_s \pi^+ \pi^-$

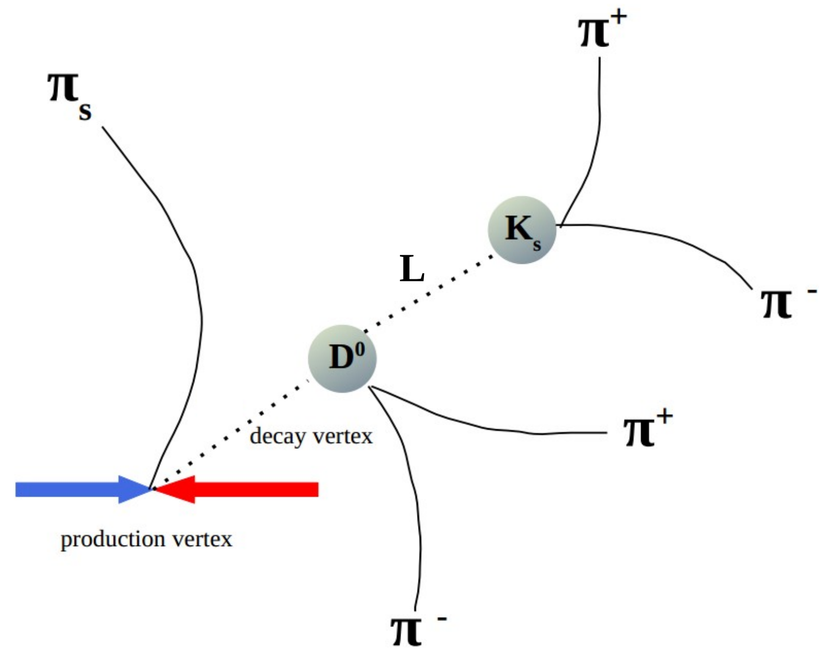


The flight distance of the $K_s$ (with respect to the $D^0$ vertex) is exploited to provide separation of the peaking background ($D^0 \rightarrow K_s\pi^+\pi^-$) from the signal ($D^0 \rightarrow K_sK_s$).

$S_{min}$ is used in the fit (no cut on $S_{min}$ is applied).

$$\boxed{\boldsymbol{S_{min} = \log(\min\ (L_i/\sigma_i))}}$$

where, $\boldsymbol{i}$ runs over the $K_s$ candidates.

# Sample Composition ($D^0 \to K_s K_s$)

| Variables | Signal | Peaking Background | Non-peaking Background |
|---|---|---|---|
| $m(D^0\pi^+)$ | 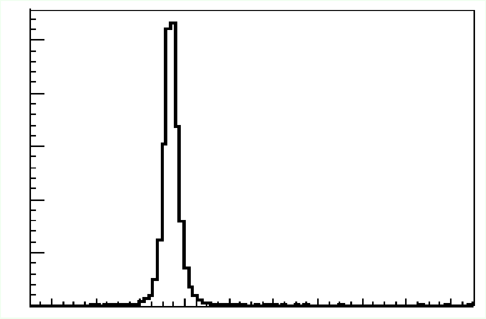 | 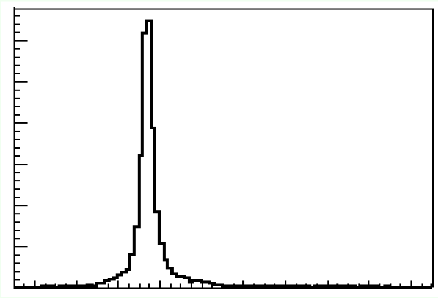 | 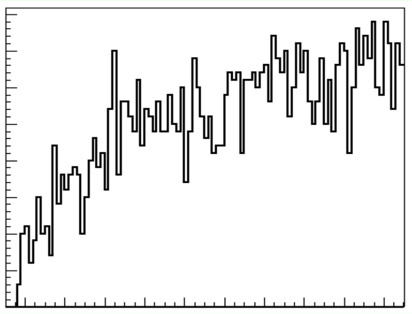 |
| $S_{min}$ | 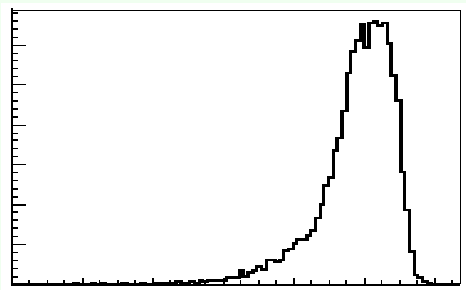 | 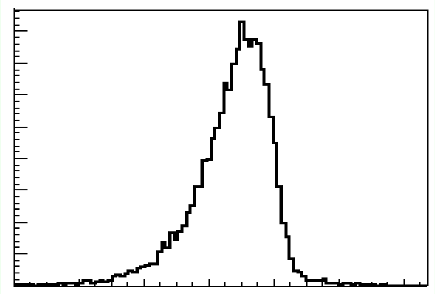 | 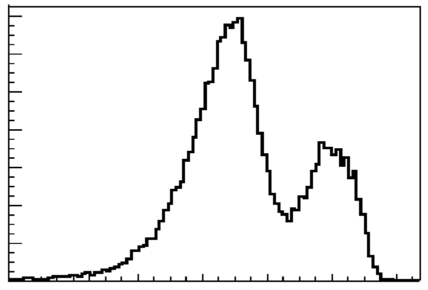 |

- Asymmetry determined from unbinned fit to ($m$, $S_{min}$) distributions of $D^0$ and $\overline{D}^0$ candidates.
- Shapes determined from either simulation or sideband data, assumed to be the same for $D^0$ and $\overline{D}^0$ decays.

# Fit projections for Belle Data

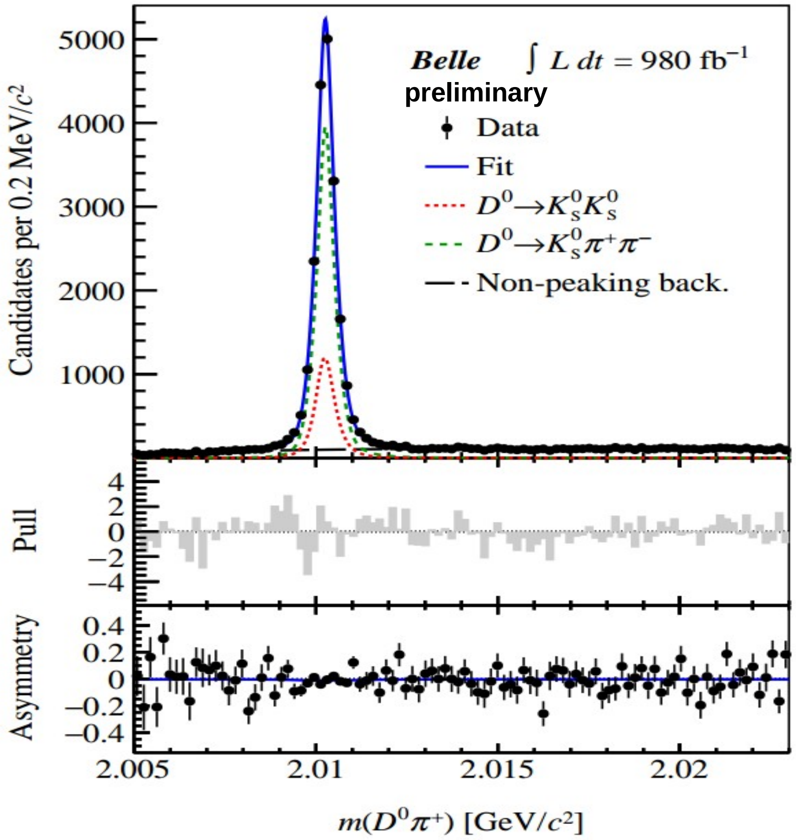


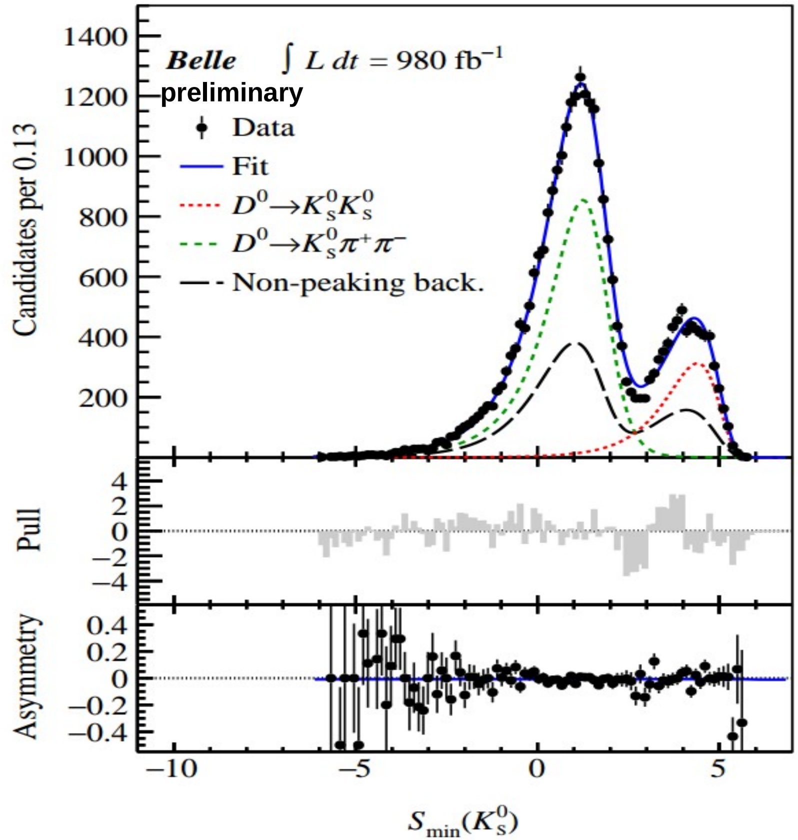


The fit model describes the data well in Belle, except in the region around $S_{min}(K^0_S) = 3.5$.

**Fit to data:**

- N ($D^0 \to K_s K_s$) = 4,864 ± 78
- $A_{raw}$ ($D^0 \to K_s K_s$) = (-1.0 ± 1.6)%

# Fit projections for Belle II Data

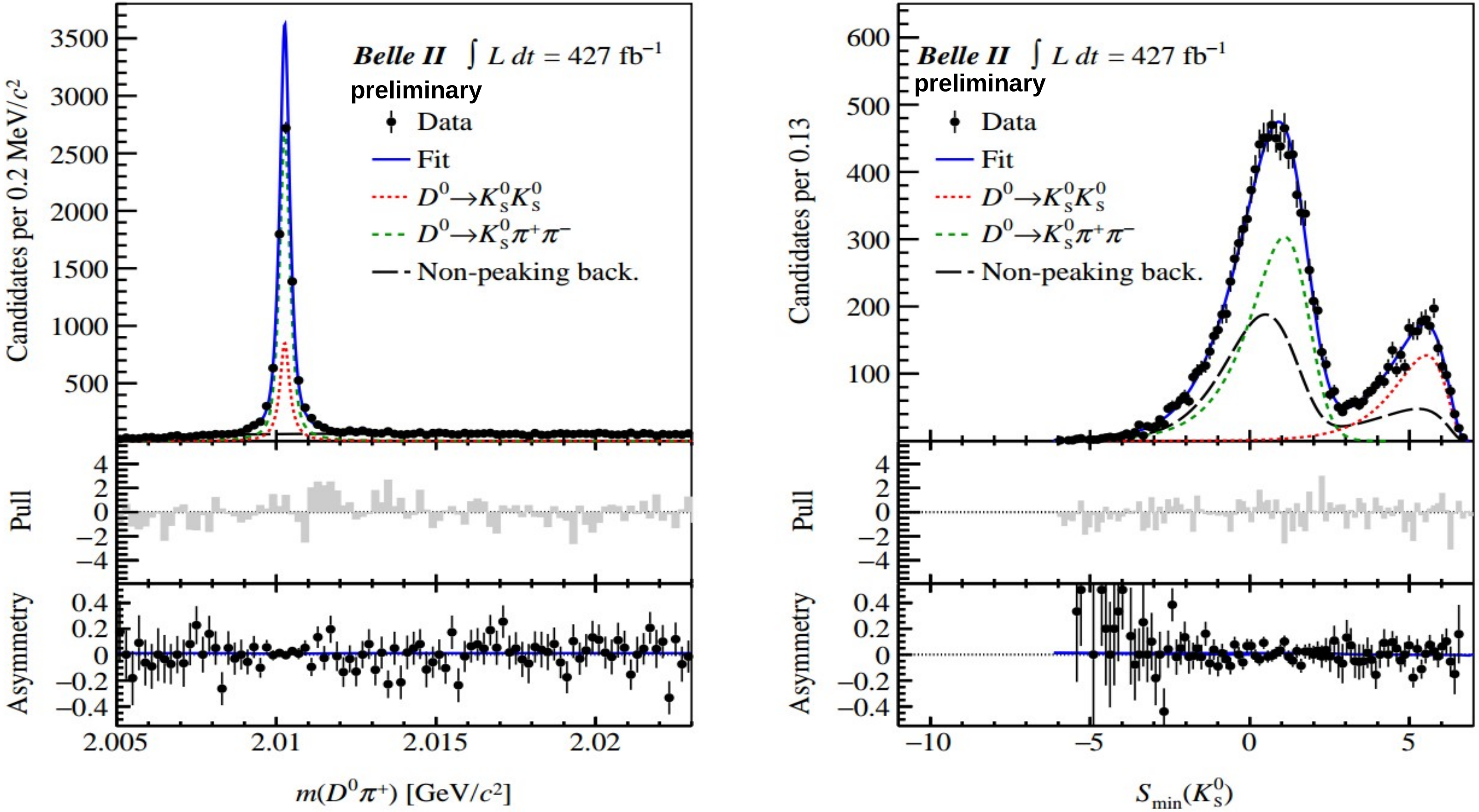


The fit model describes the data well in Belle II

- $N(D^0 \to K_s K_s) = 2{,}214 \pm 51$
- $A_{raw}(D^0 \to K_s K_s) = (-0.6 \pm 2.3)\%$

# $D^0 \to K^+K^-$ decay

## Selection Criteria

| Variable | Criteria | |
|---|---|---|
| $\lvert d_r \rvert(\pi_s^+, K^\pm)$ | $< 0.5\,\mathrm{cm}$ | (Selection criteria on Impact parameters) |
| $\lvert d_z \rvert(\pi_s^+, K^\pm)$ | $< 2\,\mathrm{cm}$ | |
| $\theta(\pi_s^+, K^\pm)$ (Belle II only) | $[17, 150]^\circ$ | |
| # CDC hits $(K^\pm)$ | $> 20$ | |
| # SVD hits $(K^\pm)$ | $> 0$ | |
| $\mathcal{L}_K/(\mathcal{L}_K + \mathcal{L}_{\pi/e})(K^\pm)$ | $0.6/0.1$ | ➡ (Identification of charged kaon from pion/electron) |
| $\Delta m$ = (m($D^{*+}$) - m($D^0$)) | $< 0.16\,\mathrm{GeV}/c^2$ | |
| $p_{\mathrm{cms}}(D^{*+})$ | $> 2.5\,\mathrm{GeV}/c$ | ➡ (To reduce the events where $D^{*+}$ coming from B meson) |
| `TreeFitter` probability | $> 0.001$ | |
| Best-candidate selection | $D^{*+}$ candidate with largest `TreeFitter` probability | |

Treefitter is used with IP constraint.

# Sample Composition ($D^0 \to K^+K^-$)

| Variables | Signal | $D^0 \to K\pi$ | $D^0 \to$ multibody (semi-leptonic, $K\pi\pi^0$) | $D_s \to KK\pi$ |
|---|---|---|---|---|
| $m(D^0\pi^+)$ | 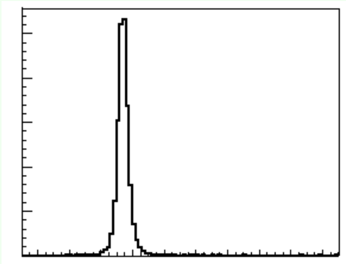 | 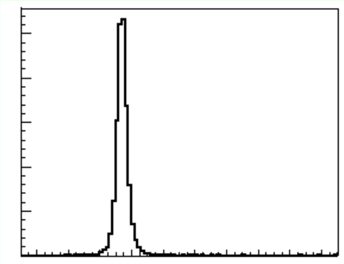 | 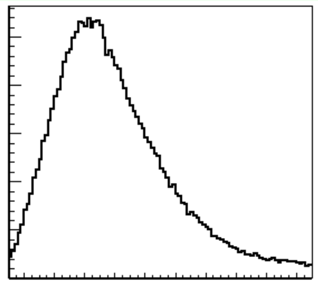 | 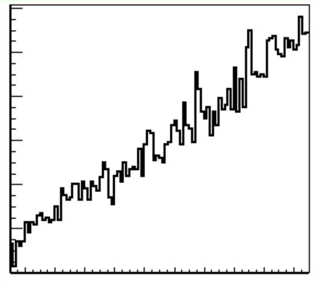 |
| $m(K^+K^-)$ | 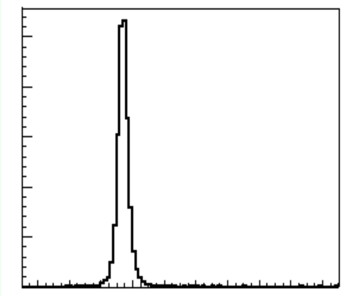 | 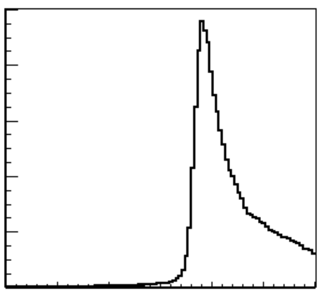 | 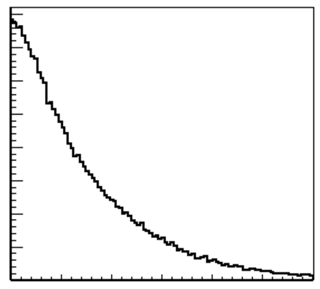 | 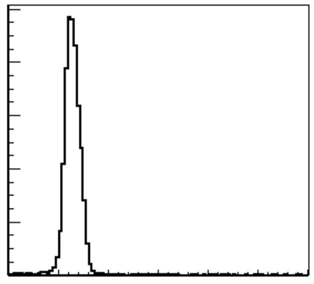 |

- Asymmetry determined from unbinned fit to ($m(D^0\pi^+)$, $m(K^+K^-)$) distributions of $D^0$ and $\overline{D}^0$ candidates.
- Shapes determined from either simulation or sideband data, assumed to be the same for $D^0$ and $\overline{D}^0$ decays.

# Distributions of momentum and cosθ for $D^{*+}$ and $\pi_s$

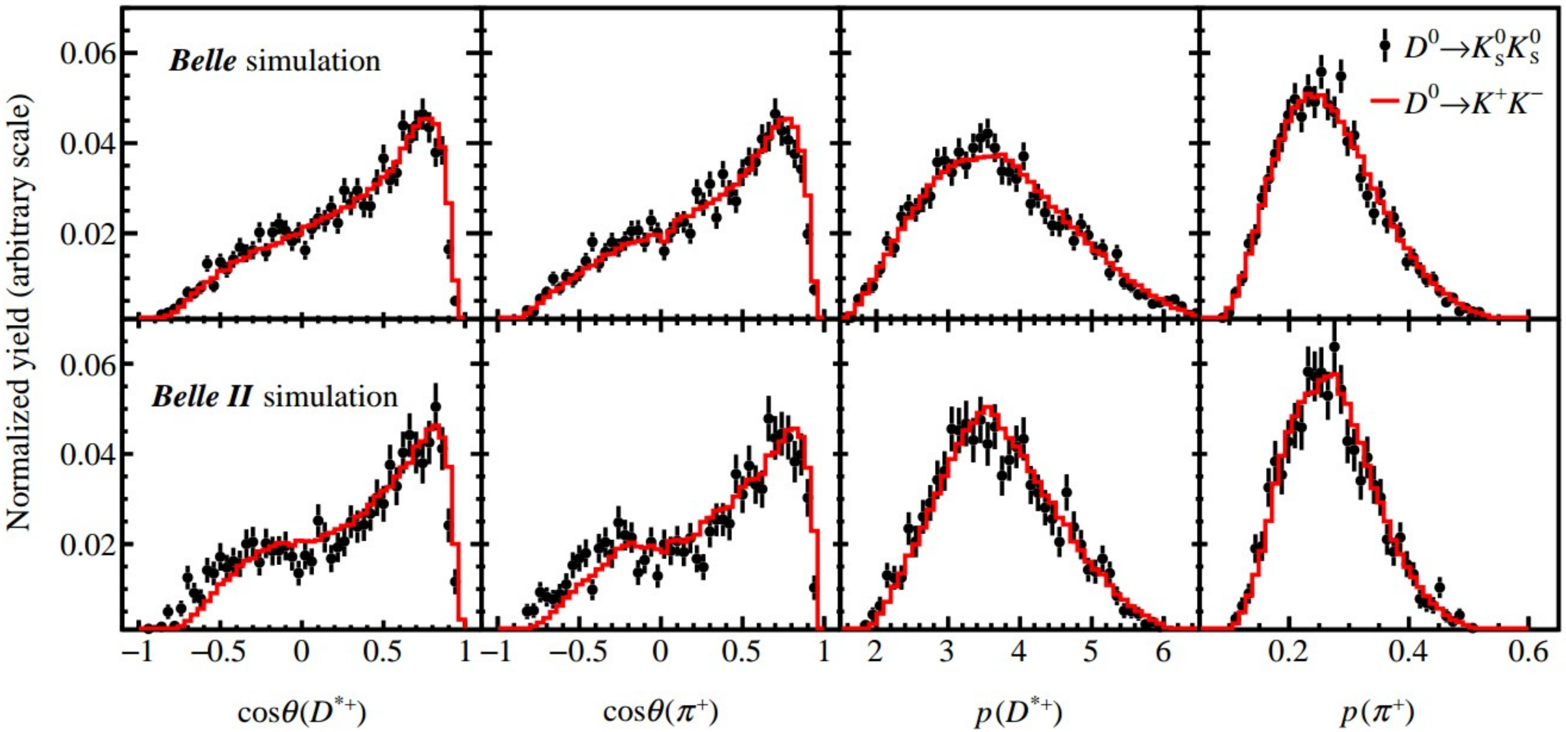


- The kinematic difference between signal and control modes in Belle II.
- Exclusively determined by the PID requirement on the charged kaons in the control mode, which imposes a reduced acceptance in the backward region due to the limited acceptance from the TOP.
- In Belle this effect is essentially absent because the PID requirement and detector acceptance are different (also due to the fact that the boost in the forward direction is larger than in Belle II).

# Fit projections for $D^0 \rightarrow K^+K^-$ (Belle)

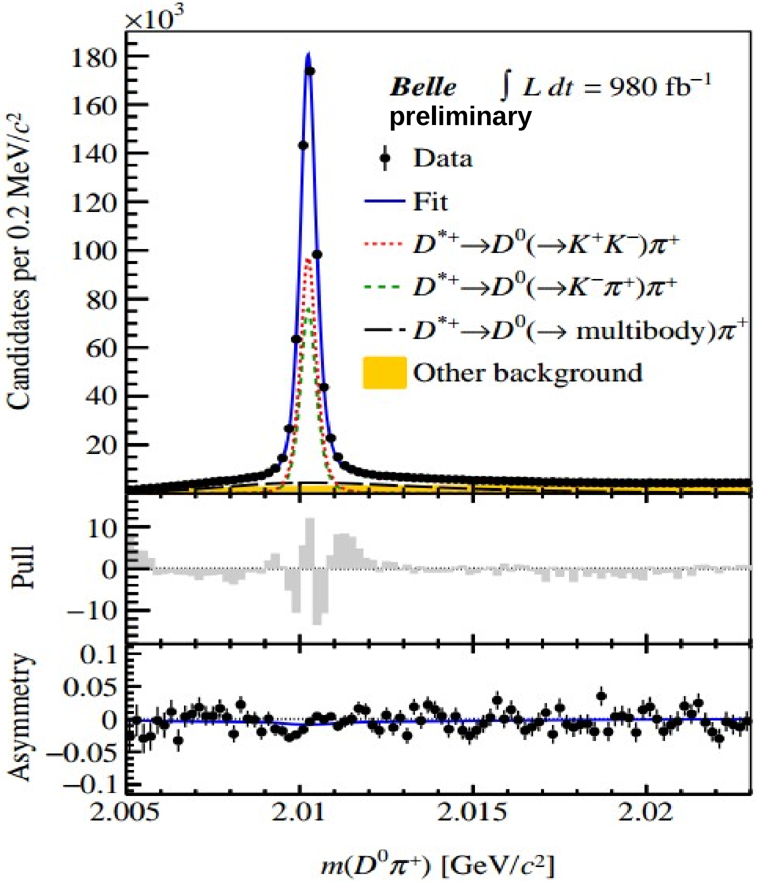


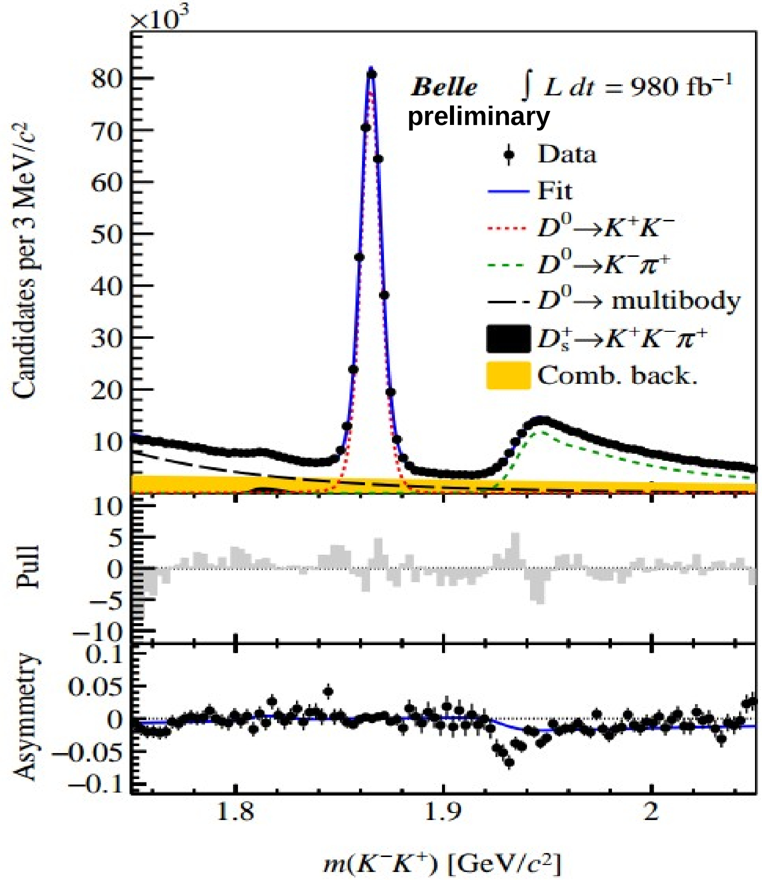


$N\,(D^0 \rightarrow K^+K^-) = 3{,}08{,}760 \pm 570$

$A_{raw}\,(D^0 \rightarrow K^+K^-) = (0.17 \pm 0.19)\%$

# Fit projections for $D^0 \to K^+K^-$ (Belle II)

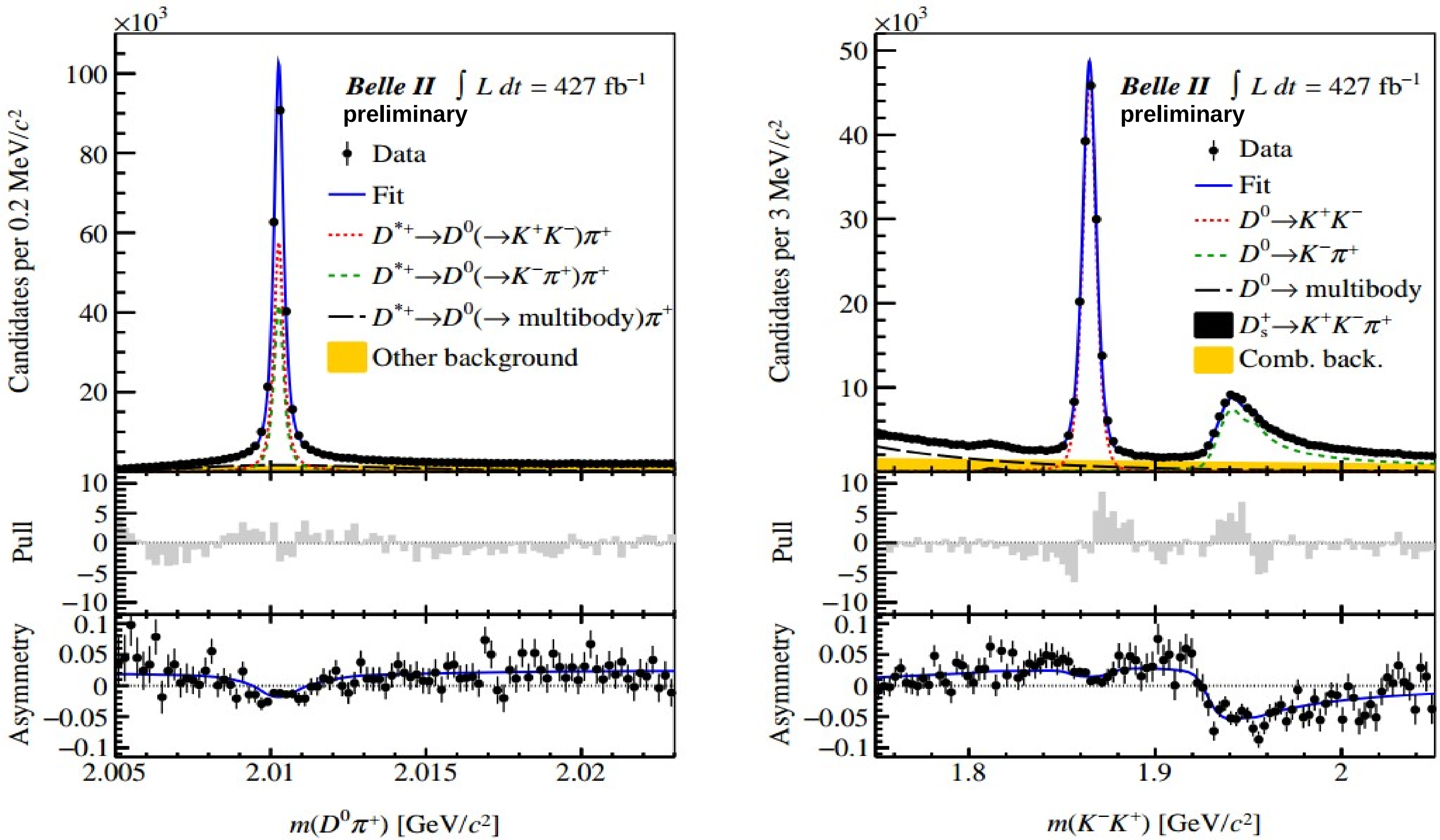


$N(D^0 \to K^+K^-) = 1,45,520 \pm 400$

$A_{raw}(D^0 \to K^+K^-) = (1.61 \pm 0.27)\%$

# Sources of systematic uncertainties in $A_{CP}(D^0 \to K_s K_s)$

- **PDF shape:**
  - Different signal and background models are tried, while the $D^0$ and $\bar{D}^0$ shapes are same.
  - Same PDFs as that of the default fit model are used, but asymmetries are introduced in the shape parameters.
- **Re-Weighting:**
  - Distributions of cosθ and momenta for $D^{*+}$ and $\pi_s$ are not in perfect agreement for the signal and control modes.
  - The difference between the weighted and unweighted fits are incorporated as a systematic.
- **$A_{CP}(D^0 \to K^+K^-)$:** External input

| Source | Uncertainty (%) Belle | Belle II |
|---|---|---|
| Modeling in the $D^0 \to K_S^0 K_S^0$ fit | 0.04 | 0.05 |
| Modeling in the $D^0 \to K^+K^-$ fit | 0.02 | $< 0.01$ |
| Kinematic equalization | 0.06 | 0.07 |
| Input $A_{CP}(D^0 \to K^+K^-)$ | 0.05 | 0.05 |
| Total systematic | 0.09 | 0.10 |
| Statistical | 1.60 | 2.30 |

## Results

$A_{CP}(D^0 \to K_s K_s)$ ***in Belle: (-1.1 ± 1.6 ± 0.1) %***

$A_{CP}(D^0 \to K_s K_s)$ ***in Belle II: (-2.2± 2.3 ± 0.1 ) %***

$A_{CP}(D^0 \to K_s K_s)$ ***(Belle + Belle II) = (-1.4 ± 1.3 ± 0.1 ) %***

first uncertainty is statistical
second is systematic.

### Comparison of $A_{cp}$ *with previous Measurements*

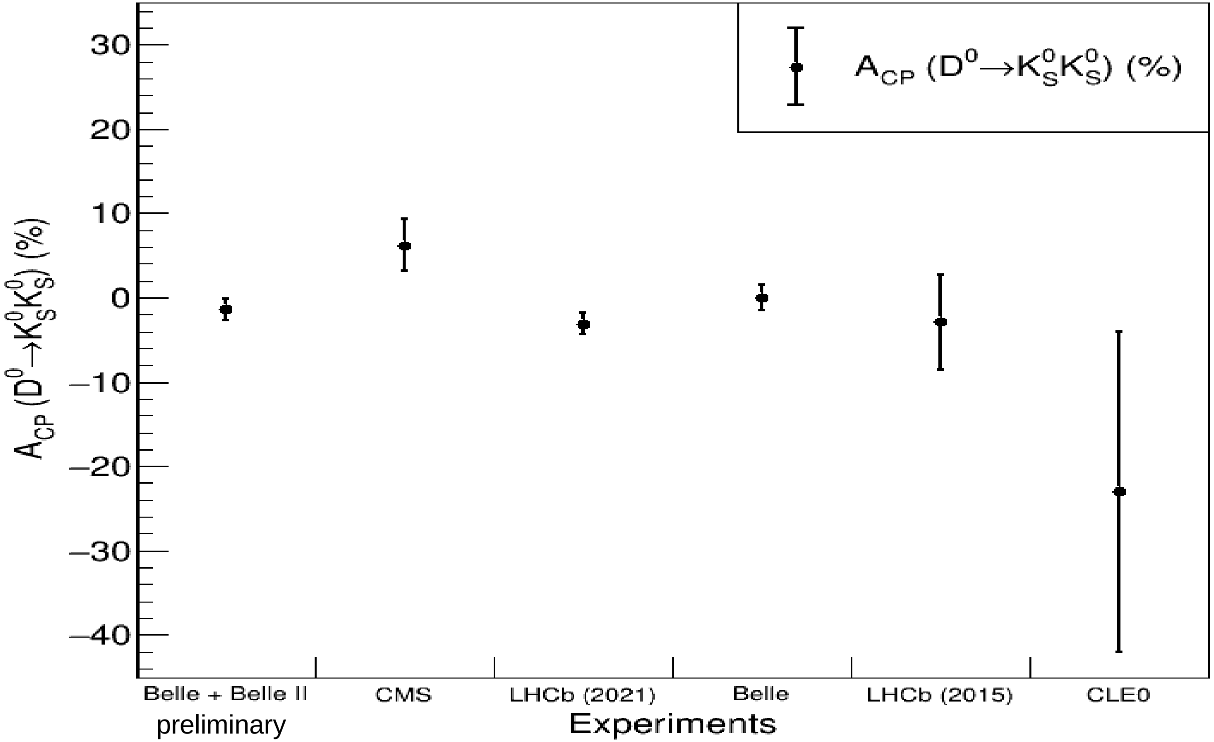


The combined results have comparable precision to the world-best measurement from LHCb.

# Summary

- Measured the $A_{CP}$ in $D^0 \to K_s K_s$ with (Belle + Belle II) dataset.

  $A_{CP}(D^0 \to K_s K_s)$ *in Belle:* $(-1.1 \pm 1.6 \pm 0.1)\ \%$

  $A_{CP}(D^0 \to K_s K_s)$ *in Belle II:* $(-2.2 \pm 2.3 \pm 0.1)\ \%$

  $\boldsymbol{A_{CP}(D^0 \to K_s K_s)}$ ***(Belle + Belle II) =*** $\boldsymbol{(-1.4 \pm 1.3 \pm 0.1)\ \%}$

- It has a factor-two better systematic uncertainty compared to the previous Belle published results, thanks to the usage of the $D^0 \to K^+K^-$ control mode, which provides a more precise $A_{CP}$ external input compared to the $D^0 \to K_S^0\pi^0$ control mode used in previous study. **Phys. Rev. Lett. 119 (2017) 171801**

- The combined results has comparable precision to the world-best measurement from LHCb.

**Thank you very much for your kind Attention**

## Back-Up Slides

| Measurement | Belle | Belle II |
|---|---|---|
| Reconstruction of B Vertex | $\sigma_z = 61$ µm | $\sigma_z = 26$ µm |
| Tracking | $\sigma_{p_t}/p_t = 0.0019\ p_t\ [\mathrm{GeV}/c\ ] \oplus 0.0030/\beta$ | $\sigma_{p_t}/p_t = 0.0011\ p_t\ [\mathrm{GeV}/c\ ] \oplus 0.0025/\beta$ |
| K$\pi$ ID | Kaon efficiency $(\epsilon_K) \approx 0.85$ with pion fake rate $(\epsilon_\pi) \approx 0.010$ for p= 2 GeV/$c$ | $\epsilon_K \approx 0.90$ with $\epsilon_\pi \approx 0.040$ for p=2 GeV/$c$ |
| Muon ID | Muon efficiency $(\epsilon_\mu) \approx 0.90$ with fake rate of muon $(\epsilon) \approx 0.020$ for p= 0.8 GeV/$c$ tracks | $\epsilon_\mu \approx$ 0.92-0.98 with, $\epsilon =$ 0.02-0.06 for p $> 1$ GeV/$c$ |
| L1 trigger | 500 Hz typical average Efficiency for hadronic events $\epsilon_{hadron}\approx 1$ | 30 kHz max. average rate $\epsilon_{hadron}\approx 1$ |
| DAQ | $\approx 5\%$ dead time at 500 Hz L1 rate | $< 3\%$ dead time at 30 kHz L1 rate |

Table 2.1: Comparison of the performance metrics of Belle with Belle II [46].

# Fit Models for D->KsKs

mation, the 2D probability distribution function (PDF) of each component factorizes into the product of the two 1D PDFs,

$$\mathrm{pdf}^i(\Delta m, \gamma) = \mathrm{pdf}^i(\Delta m)\mathrm{pdf}^i(\gamma) \qquad (i = K^0_S K^0_S, K^0_S\pi\pi, \mathrm{bkg}) \,, \tag{6}$$

and that no substantial differences are observed between PDFs of $D^0$ and $\overline{D}^0$ decays, which are then assumed to be identical (Appendix A). Possible asymmetries in the PDFs shapes are tested in the systematic studies, as discussed in Section 5.1.

The PDFs for the signal and peaking background component are derived using simulation. For signal, each of the $\Delta m$ and $\gamma$ distributions is modeled using a Johnson's $S_U$ function [21]

$$J(x|\mu_J, \lambda_J, \delta_J, \gamma_J) \propto \frac{e^{-\frac{1}{2}\left[\gamma_J \;+\; \delta_J \;\sinh^{-1}\left(\frac{x-\mu_J}{\lambda_J}\right)\right]^2}}{\sqrt{1+\left(\frac{x-\mu_J}{\lambda_J}\right)^2}} \,, \tag{7}$$

as shown in Figure 4.

The $\Delta m$ PDF of the $D^0 \to K^0_S\pi^+\pi^-$ background is modelled using the sum of a Johnson's $S_U$ and a Gaussian function with a common mean parameter for the Belle II analysis, while for the Belle Analysis, it is modelled only with a Johnson 's $S_U$ function,

$$\mathrm{pdf}^{K^0_S\pi^+\pi^-}(\Delta m) = f_J\, J(\Delta m|\mu_J, \lambda_J, \delta_J, \gamma_J) + (1-f_J)G(\Delta m|\mu_J, \sigma_G) \,. \tag{8}$$

The $\gamma$ is modelled using a Johnson's $S_U$ function. The distributions resulting from the fits to truth-matched $D^0 \to K^0_S\pi^+\pi^-$ background in simulation are shown in Figure 5.

The $\Delta m$ PDF of the non-peaking background is modeled empirically as a threshold-like distribution,

$$\mathrm{pdf}^{\mathrm{bkg}}(\Delta m) \propto (\Delta m - \Delta m_0)^{1/2} + \alpha(\Delta m - \Delta m_0)^{3/2} + \beta(\Delta m - \Delta m_0)^{5/2} \tag{9}$$

with threshold parameter $\Delta m_0$ fixed to the known value of the charged pion mass [20]. The value of the parameters $\alpha$ and $\beta$ are determined directly from the fit to the data. The $\gamma$ distribution is modeled as the sum of two Johnson $S_U$ functions using data candidates populating the $\Delta m$ sideband region $[0.14, 0.143]\cup[0.148, 0.158]$ GeV/$c^2$ (Figure 6). We have tested on simulation that this sideband reproduces the distribution of the non-peaking background in the signal region (Appendix A).

Omitting the arguments to simplify the notation, the total fit function is

$$\begin{aligned} f^q(\Delta m, \gamma) = N^{K^0_S K^0_S}\,(1 + qA^{K^0_S K^0_S}_{\mathrm{raw}})\,\mathrm{pdf}^{K^0_S K^0_S} \\ + N^{K^0_S\pi\pi}\,(1 + qA^{K^0_S\pi\pi}_{\mathrm{raw}})\,\mathrm{pdf}^{K^0_S\pi\pi} \\ + N^{\mathrm{bkg}}\,(1 + qA^{\mathrm{bkg}}_{\mathrm{raw}})\,\mathrm{pdf}^{\mathrm{bkg}} \,, \end{aligned} \tag{10}$$

where $q = 1$ $(-1)$ for $D^0$ $(\overline{D}^0)$ candidates and $N^i$ and $A^i_{\mathrm{raw}}$ are, respectively, the total yield and the raw asymmetry of the component $i$. The parameter $\alpha$ of the background is only shape parameter left free in the fit, together with the yields and asymmetries. All other parameters are fixed to their values as determined on simulation or data sideband.

# Fit Models for D->KK (control mode)

The raw asymmetry of the control decays is determined using an unbinned (and extended) fit to the two-dimensional $(m(K^+K^-), m(D^0\pi_s))$ distribution of $D^0$ and $\overline{D}^0$ candidates. The fit considers the $D^{*+} \to D^0(\to K^+K^-)\pi^+$ and all the background components discussed in the previous section. Simulation shows that 2D PDF of each component, except for the $D_s^+ \to K^+K^-\pi^+$ background, can be approximated into the product of the two 1D PDFs,

$$\mathrm{pdf}^i(m(K^+K^-), m(D^0\pi_s)) = \mathrm{pdf}^i(m(K^+K^-))\mathrm{pdf}^i(m(D^0\pi_s)) \qquad (i = K^+K^-, ...)\,, \quad (13)$$

and that no substantial differences are observed between PDFs of $D^0$ and $\overline{D}^0$ decays, which are then assumed to be identical (Appendix A). Possible asymmetries in the PDFs shapes are tested in the systematic studies, as discussed in Section 5.2.

The control decays and physics backgrounds PDFs are determined in simulation using truth matching. The $m(K^+K^-)$ and $m(D^0\pi_s)$ PDFs of the $D^{*+} \to D^0(\to K^+K^-)\pi^+$ decays are each modelled using the sum of two Gaussian functions (with a common mean) and of a Johnson's $S_U$ function (Figure 22),

$$\begin{aligned}\mathrm{pdf}^{K^+K^-}(m) = {}& f_J\, J(m|\mu_J, \lambda_J, \delta_J, \gamma_J) + \\ & + (1 - f_J)\left[f_{G1} G(m|\mu_{G1}, \sigma_{G1}) + (1 - f_{G1}) G(m|\mu_{G1}, \sigma_{G2})\right]\,, \quad (14)\end{aligned}$$

with $m$ being either $m(K^+K^-)$ or $m(D^0\pi_s)$.

# Fit Models for D->KK (control mode)

The $m(K^+K^-)$ PDF of the mis-identified $D^{*+} \to D^0(\to K^-\pi^+)\pi^+$ background is parametrized using the sum of a Gaussian and a Johnson's $S_U$ function as shown in Figure 23. Given that $m(D^0\pi_s)$ is unaffected by the mis-assigned mass hypothesis to the $D^0$ final state particles, the $m(D^0\pi_s)$ PDF is shared with that of the control decays.

The partially reconstructed $D^{*+} \to D^0(\to \text{multibody})\pi^+$ decays are modeled as an exponential function in $m(K^+K^-)$ and as a Johnson's $S_U$ function, with parameter $\gamma_J$ fixed to unity, in $m(D^0\pi_s)$ (Figure 24).

For each of the aforementioned components there is a corresponding one in which an unrelated soft pion is associated with the identified $D^0$ candidate. These random pions components (indicated as $K^+K^-$ rnd, $K\pi$ rnd, and mult rnd) share the same $m(K^+K^-)$ distribution as the component with the correctly reconstructed soft pion and are modeled in $m(D^0\pi_s)$ with PDF derived directly from the fit to the data:

$$\mathrm{pdf}^{i\,\mathrm{rnd}}(m|m_0, A, B, C) = \left(1 - \exp\left(-\frac{m-m_0}{C}\right)\right) \cdot \left(\frac{m}{m_0}\right)^A + B\left(\frac{m}{m_0} - 1\right), \qquad (15)$$

where $m = m(D^0\pi_s)$ and $m_0 = m_D^0 + m_\pi^+ = 2.00441\,\mathrm{GeV}/c^2$ denotes the $m(D^0\pi_s)$ threshold.

The $D_s^+ \to K^+K^-\pi^+$ background in which the pion acts as the soft pion exhibits a kinematic correlation between $m(D^0\pi_s)$ and $m(K^+K^-)$ which can be calculated analytically as (Figure 25)

$$\langle m(K^+K^-)\rangle\,(m(D^0\pi_s)) = m_{D_s^+} + m_{D^0} - m(D^0\pi_s) = 3.83319\,\mathrm{GeV}/c^2 - m(D^0\pi_s)\,, \quad (16)$$

using the known $D_s^+$ and $D^0$ masses [20]. The two-dimensional PDF is written as the product of the $m(K^+K^-)$ PDF, conditional to the value of $m(D^0\pi_s)$, and of the $m(D^0\pi_s)$ PDF,

$$\mathrm{pdf}^{D_s^+}(m(K^+K^-), m(D^0\pi_s)) = \mathrm{pdf}^{D_s^+}(m(K^+K^-)|m(D^0\pi_s))\,\mathrm{pdf}^{D_s^+}(m(D^0\pi_s))\,. \qquad (17)$$

The first term is parametrized as a Johnson's $S_U$ function with mean parameter given by $\mu_J + \langle m(K^+K^-)\rangle\,(m(D^0\pi_s))$. An offset with respect to the analytical $\langle m(K^+K^-)\rangle$, $\mu_J$, is used to account for possible data-simulation differences in the peak positions. The $m(D^0\pi_s)$ PDF is a first-order polynomial defined only about the threshold value of $m_D^0 + m_\pi^+$ [20]. The obtained distributions when fitting truth-matched decays are shown in Figure 26.

Finally, the purely combinatorial background is described as a linear function in $m(K^+K^-)$ and as a random-pion background in $m(D^0\pi_s)$. The $m(D^0\pi_s)$ parametrization this component is shared with that of the other random-pion components.

Omitting the arguments to simplify the notation, the total fit function is

$$\begin{aligned} f = {} & N^{K^+K^-}(1 + qA_{\mathrm{raw}}^{K^+K^-})\,\mathrm{pdf}^{K^+K^-} + N^{K^+K^-\,\mathrm{rnd}}(1 + qA_{\mathrm{raw}}^{K^+K^-\,\mathrm{rnd}})\,\mathrm{pdf}^{K^+K^-\,\mathrm{rnd}} \\ & + N^{K\pi}(1 + qA_{\mathrm{raw}}^{K\pi})\,\mathrm{pdf}_{K\pi} + N^{K\pi\,\mathrm{rnd}}(1 + qA_{\mathrm{raw}}^{K\pi\,\mathrm{rnd}})\,\mathrm{pdf}^{K\pi\,\mathrm{rnd}} \\ & + N^{\mathrm{mult}}(1 + qA_{\mathrm{raw}}^{\mathrm{mult}})\,\mathrm{pdf}^{\mathrm{mult}} + N^{\mathrm{mult\,rnd}}(1 + qA_{\mathrm{raw}}^{\mathrm{mult\,rnd}})\,\mathrm{pdf}^{\mathrm{mult\,rnd}} \\ & + N^{D_s^+}(1 + qA_{\mathrm{raw}}^{D_s^+})\,\mathrm{pdf}^{D_s^+} + N^{\mathrm{comb}}(1 + qA_{\mathrm{raw}}^{\mathrm{comb}})\,\mathrm{pdf}^{\mathrm{comb}} \qquad (18) \end{aligned}$$

How to calculate weight to correct the discrepency in costheta and momenta of D*+ and soft pion?

## 4.2 Kinematic equalization

The $D^{*+}$ forward-backward asymmetry is expected to vary as a function the $D^{*+}$ polar angle.[4] The $\pi_s$ detection asymmetry is expected to vary both as a function of momentum and of polar angle. To ensure a precise cancellation of these nuisance asymmetries in Equation (4), the $D^{*+}$ and $\pi_s$ kinematic distributions of the control sample must coincide with those of the signal sample. We expect these differences to be mostly due to the differing acceptance introduced by the PID requirements. PID is used only for the control mode, so the most backward region of the detector (which is covered only by the CDC and not by the TOP) cannot accept $D^0 \to K^+K^-$ decays while it can accept $D^0 \to K_S^0 K_S^0$ decays. The effect is more evident in Belle II compared to Belle because of the smaller boost.

Simulation shows that, because of the different selection criteria, small differences are present (Figures 14 and 15). A weighting procedure is therefore implemented to reduce the observed differences. We fit a six-order polynomial to the ratio between the $\cos\theta(D^{*+})$ distributions of truth-matched $D^0 \to K_S^0 K_S^0$ and $D^0 \to K^+K^-$ decays in simulation. The

[4] Neglecting possible efficiency effects, because of the $CP$ symmetric initial state, the forward-backward asymmetry is expected to be an odd function of the cosine of the polar angle in the c.m.s.

projections of the fit are shown in Figures 14 and 15. The resulting functions,

$$f(\cos\theta) = 0.984751 - 0.13327\cos\theta + 0.276899\cos^2\theta + 0.453082\cos^3\theta - 0.08738\cos^4\theta - 1.00713\cos^5\theta \quad (11)$$

for Belle and

$$f(\cos\theta) = 0.889752 - 0.110344\cos\theta + 0.961291\cos^2\theta - 0.220356\cos^3\theta - 0.0826763\cos^4\theta - 3.09148\cos^5\theta + 2.45831\cos^6\theta \quad (12)$$

for Belle II, are used to compute a per-candidate weight for the $D^0 \to K^+K^-$ control sample. The effect of the weighting on simulated and truth-matched control sample decays is shown in Figures 16 and 17. Weighting as a function of $\cos\theta(D^{*+})$ reduces the differences also in the other kinematic distribution.

To check that the weighting functions determined on simulation work also on data (Figures 18 and 19), we evaluate the effect of the weighting procedure on background-subtracted signal and control decays in data. The background subtraction is performed using the sPlot method [23] with weights derived from the fits discussed in Section 4.3. Figures 20 and 21 show the results, confirm that the weighting functions from simulation are effective also in data.

$$A_{raw}^{KK} = \cancel{A_{FB}^{\vartheta KK}} + A_{CP}^{KK} + \cancel{A_{\varepsilon}^{\pi_s KK}} \rightarrow (i)$$

$$A_{raw}^{K_sK_s} = \cancel{A_{FB}^{\vartheta K_sK_s}} + A_{CP}^{K_sK_s} + \cancel{A_{\varepsilon}^{\pi_s K_sK_s}} \rightarrow (ii)$$

→ assuming these cancel

So (i) − (ii),

$$A_{raw}^{KK} - A_{raw}^{K_sK_s} = A_{CP}^{KK} - A_{CP}^{K_sK_s}$$

$$\Rightarrow \boxed{A_{CP}^{K_sK_s} = \left(A_{raw}^{K_sK_s} - A_{raw}^{KK}\right) + A_{CP}^{KK}}$$